Multispectral imaging: narrow or wide band filters?

Xingbo Wang[1,2], Jean-Baptiste Thomas[1], Jon Y Hardeberg[2] and Pierre Gouton[1]

[1]*Laboratoire Electronique, Informatique et Image, Université de Bourgogne, France*
[2]*The Norwegian Colour and Visual Computing Laboratory, Gjøvik University College, Norway*
Email: xingbo.wang@hig.no

In every aspect, spectral characteristics of filters play an important role in an image acquisition system. For a colorimetric system, traditionally, it is believed that narrow-band filters give rise to higher accuracy of colour reproduction, whereas wide-band filters, such as complementary colour filters, have the advantage of higher sensitivity. In the context of multispectral image capture, the objective is very often to retrieve an estimation of the spectral reflectance of the captured objects. The literature does not provide a satisfactory answer to which configuration yields the best results. It is therefore of interest to verify which type of filters performs the best in estimating the reflectance spectra for the purpose of multispectral image acquisition. A series of experiments were conducted on a simulated imaging system, with six types of filters of varying bandwidths paired with three linear reflectance estimation methods. The results show that filter bandwidth exerts direct influence on the accuracy of reflectance estimation. Extremely narrowband filters did not perform well in the experiment and the relation between bandwidth and reflectance estimation accuracy is not monotonic. Also it is indicated that the optimal number of filters depends on the spectral similarity metrics employed.

Received 19 June 2014; accepted 20 June 2014

Published online: 15 July 2014

Introduction

In practice, a multiband image acquisition system often employs an objective lens, a set of optical filters and an area image sensor with the aim of recording the projected image of a scene captured by the system. Each filter corresponds to one band of the resulting multiband image, and a subsequent estimation step is commonly required in order to retrieve the CIE tristimulus values or spectral reflectance of the scene.

Filter design is the very first component of such a system. Spectral characteristics of filters therefore make a direct impact on the overall performance of the system. When simplified as a normal (Gaussian) distribution, a filter can be described primarily by two factors, i.e., central wavelength and bandwidth. The former specifies the dominating wavelength where the transmittance of a filter achieves the maximum, and the latter determines how the filter respond to the incident light distributed among the remaining part of the spectrum. The bandwidth of a filter is commonly measured by Full Width at Half Maximum (FWHM).

In case of a trichromatic system, three types of colour recording filters are often required. Primary colour filters whose peak transmittances are located in the blue, green and red region of the visible spectrum are commonplace in commercial colour cameras [1]. However, there exist colour cameras that possess complementary colour filters in contrast to the primary colour filters commonly utilised. Complementary colour filters intrinsically bear wider pass-band than their primary counterparts, and it is demonstrated that the former gives rise to better colour reproduction and signal-to-noise ratio in sufficient lighting conditions, whereas the latter offers higher sensitivity and resolution [2, 3]. Similarly, the choice of filters remains a question in multispectral capture. It is stated that narrowband filters should in theory outperform wideband ones with respect to the accuracy of spectral reconstruction [4, 5], whereas the wideband filters may produce superior results [4]. To the best of our knowledge, little research has been made so far to investigate the influence of various filter bandwidths on multispectral acquisition.

In this context, our previous research on multispectral demosaicking [6, 7] posed the question of filter design in relation to the inter-band correlation, and consequently we presented some preliminary results [8]. In this paper, we focus on the impact of filter bandwidth on the accuracy of spectral reflectance estimation in the context of a multispectral image acquisition system, in a comprehensive and rigorous manner.

The following parts of the article are organised as follows. It begins by a description of three linear reflectance reconstruction methods that are widely adopted and used. Next the procedures of and conditions in which the experiments were conducted are introduced prior to a presentation of the results. The last section draws some conclusions.

Methods of spectral reflectance estimation from multispectral measurements

Spectral reflectance estimation is an inverse problem aimed at an estimation of the spectra of higher dimensions from the corresponding multispectral measurements of lower dimensions. In concrete terms, a multispectral capture process can be described in a linear form as

$$\mathbf{p} = \mathbf{SEr} \qquad (1)$$

where $\mathbf{p}$ refers to the multispectral responses represented by a $m \times k$ matrix, $\mathbf{S}$ corresponds to system responsivities represented by a $m \times n$ matrix, $\mathbf{E}$ is the spectral power distribution of the illumination represented by a $n \times n$ matrix, and $\mathbf{r}$ is the incoming spectra represented by a $n \times k$ matrix, where m is the number of spectral bands captured by the system, n is number of spectral components of incident spectra, and k is the number of spectra. For multispectral image capture $m > 3$, whereas trichromatic acquisition can be considered as a special case where $m = 3$.

Spectral reflectance estimation aims at an estimation of $\mathbf{r}$ from $\mathbf{p}$. Equation 1 is solvable if $\mathbf{SE}$ is known and invertible, so that we have $\mathbf{r}' = \mathbf{Wp}$ where $\mathbf{W} = (\mathbf{SE})^{-1}$. However it is not true in the case of

reflectance reconstruction. Nevertheless $\mathbf{W}$ can be estimated by means of training where a collection of training spectra $\mathbf{r}_t$ and corresponding responses $\mathbf{p}_t$ are utilised to derive an approximation of $\mathbf{W}$. Three representative methods based on different principles were experimented with to this end.

The method of linear least squares attempts to solve (1) by means of least-squares which leads to Equation 2:

$$\mathbf{W} = \mathbf{r}_t\mathbf{p}_t^+ \tag{2}$$

where $\mathbf{p}_t^+$ is a right pseudoinverse of $\mathbf{p}_t$: $\mathbf{p}_t^+ : \mathbf{p}_t^T(\mathbf{p}_t\mathbf{p}_t^T)^{-1}$.

Imai and Berns [9] proposed to employ PCA (principal component analysis) to analyse the training spectra, which gives rise to Equation 3:

$$\mathbf{W} = \boldsymbol{u}_l\mathbf{p}_t^+ \tag{3}$$

where $\boldsymbol{u}$ is a $n \times l$ matrix consisting of the l most significant eigenvectors of the training spectra by means of PCA. The parameter l is determined so that the RMSE (root mean square error) between $\mathbf{r}_t$ and the estimated $\mathbf{r}_t'$ is minimised.

Wiener estimation [10] is yet another method taking noise into consideration in the following manner,

$$\mathbf{W} = \mathbf{r}_t\mathbf{r}_t^T(\mathbf{SE})^T((\mathbf{SE})\mathbf{r}_t\mathbf{r}_t^T)(\mathbf{SE})^T + \mathbf{N})^{-1} \tag{4}$$

where $\mathbf{N}$ is a term reflecting additive noise intrinsic to the system in form of $\sigma^2\mathbf{I}$, σ^2 being the variance of estimated noise and $\mathbf{I}$ being an identity matrix. σ^2 is estimated using the method proposed by Hironaga and Shimano [10].

Experimental setup

The experiments were conducted on an experimental platform that simulates key elements of a CFA/MSFA based multispectral imaging system. To avoid unnecessary steps, off-the-shelf hyperspectral images are employed as the irradiance image formed by the optical system in the image plane after integrated by the sensor that bears as many pixels as the images themselves.

In total 48 hyperspectral images were used in this study. 16 of them from Foster's database [11] consist of a mixture of rural scenes, and another 32 from the CAVE project [12] include a wide variety of real-world materials and objects and artificial replicas. Spectral reflectance images were derived respectively and re-lit by the illuminant of CIE D65. A selection of pixel was selected from each image by means of horizontal and vertical down-sampling at the ratio of 1:5 without low-pass filtering, in order to reduce the computational intensity.

For the ease of processing and comparison, all images were interpolated spectrally, and filters were designed accordingly, to cover the range between 400 nm and 700 nm with an interval of 1 nm.

We chose six types of filter sets in three pairs. A 4-band filter set used in this research are depicted in Figure 1. We were interested in narrowband and wideband band-pass filters as well as corresponding inverted ones as band-stop filters. The FWHM of pass-band and stop-band was set to 10/40/160 nm respectively. In practice, a pass-band of 10 nm simulates very narrow band-pass filters like LCTF (Liquid Crystal Tunable Filter), a stop-band of 10 nm mimics notch filters relying on

destructive interference. Similarly, a pass-band and a stop-band of 40/160 nm resemble the spectral transmittances of thin-film absorptive filters. The peak wavelengths were determined so that the intersection between both ends of the spectrum and the 40 nm band-pass filters correspond to the 3σ location, namely the filters cover the short end and long end of the spectrum with rather low transmittances. The number of filters studied ranged from 3 to 20.

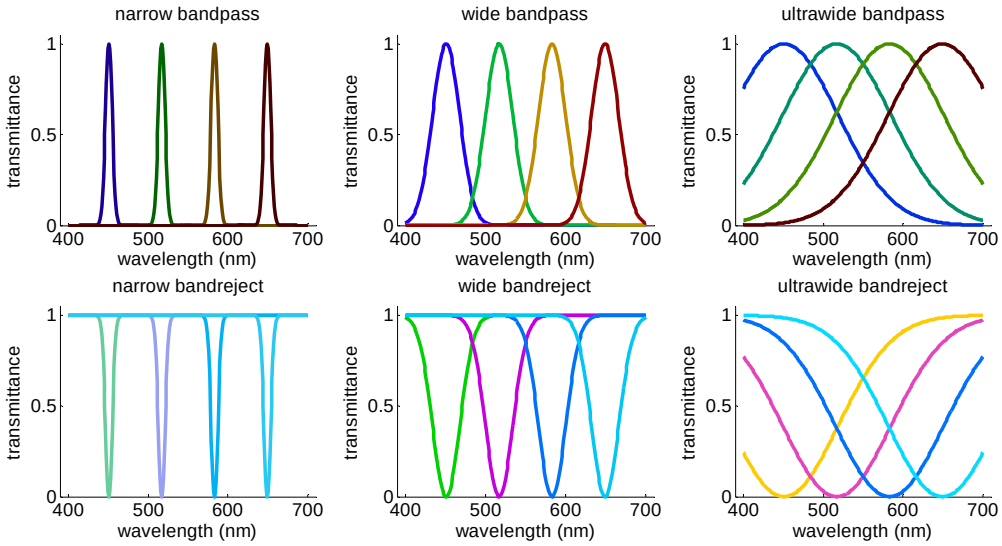

Figure 1: An example set of 4-band filters. The three graphs in the upper row show narrow, wide and ultra-wide band-pass filters' spectral transmittances with FWHM of 10, 40 and 160 nm respectively. The three drawings in the lower row present spectral transmittances of the corresponding band-reject filter sets.

To make the results more robust and realistic, we also introduced a certain level of normally distributed noise to the simulated sensor responses. The mean level was determined so that the maximum signal-to-noise ratio (SNR) is 50 dB with the standard deviation at 10% of the noise level.

To simplify the simulation, we also made an approximation that the sensor possesses constant quantum efficiency over the spectrum.

The influence of the above filters in terms of the spectrum estimation accuracy was evaluated by means of Root Mean Square Error (RMSE) and Goodness of Fit Coefficient (GFC) [13] averaged among the 48 virtual scenes, as indicated underneath by Equations 5 and 6.

$$\mathrm{GFC} = \frac{\left|\sum_{j=1}^{301} R(\lambda_j) R'(\lambda_j)\right|}{\left|\sum_{j=1}^{301} \left[R(\lambda_j)\right]^2\right|^{1/2} \left|\sum_{j=1}^{301} \left[R'(\lambda_j)\right]^2\right|^{1/2}} \tag{5}$$

$$\mathrm{RMSE} = \sqrt{\frac{\sum_{j=1}^{301} \left[\left|R(\lambda_j) - R'(\lambda_j)\right|^2\right]}{301}} \tag{6}$$

where R and R' represent the original and estimated spectral reflectance at any pixel in an image. It is worth noting that lower RMSE scores mean higher performance and an RMSE of zero means a perfect estimation, whereas, GFC values range from 0 to 1 and an exact reconstruction would yield 1.

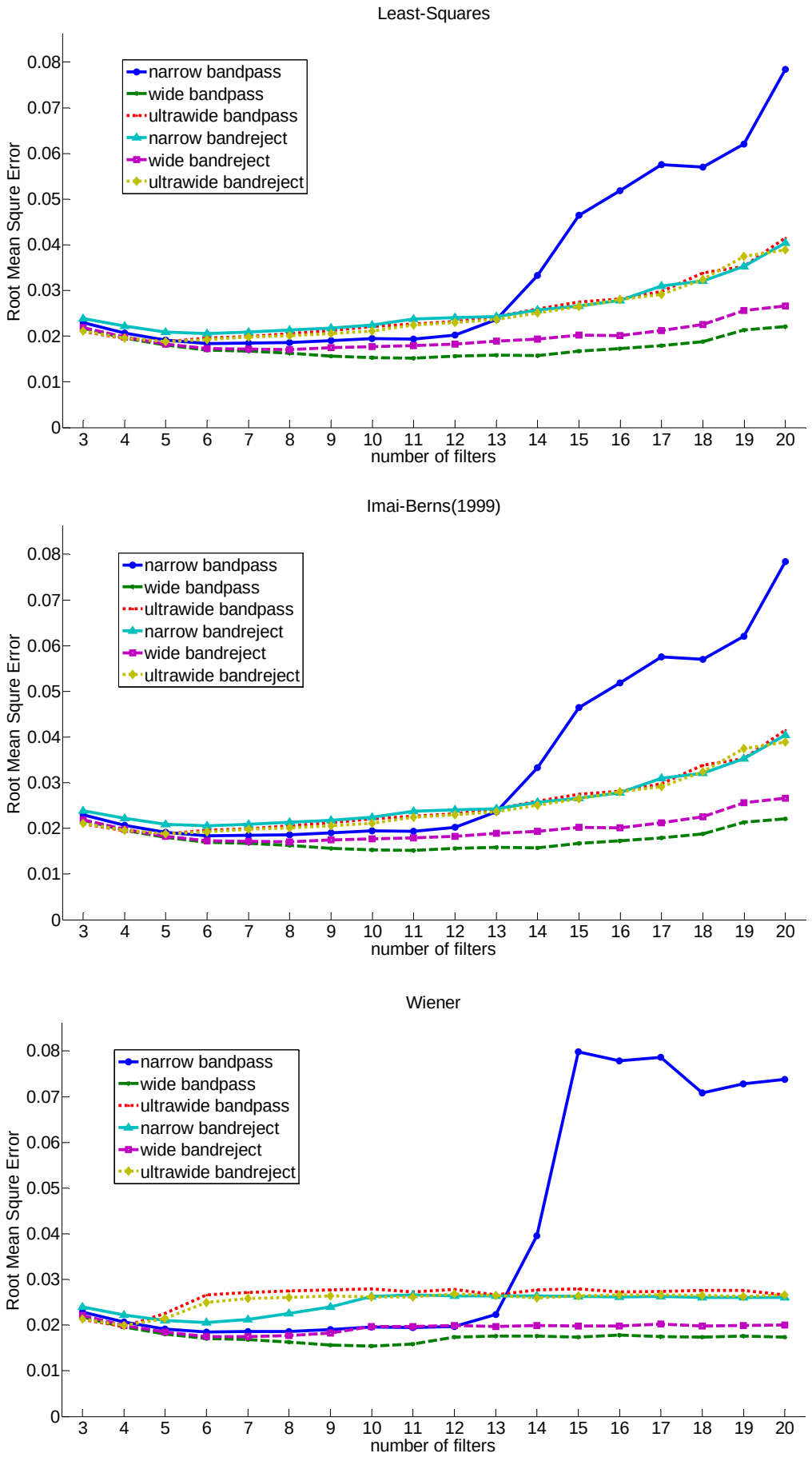

Figure 2: Accuracy of spectrum estimation evaluated by Root Mean Square Error (RMSE).

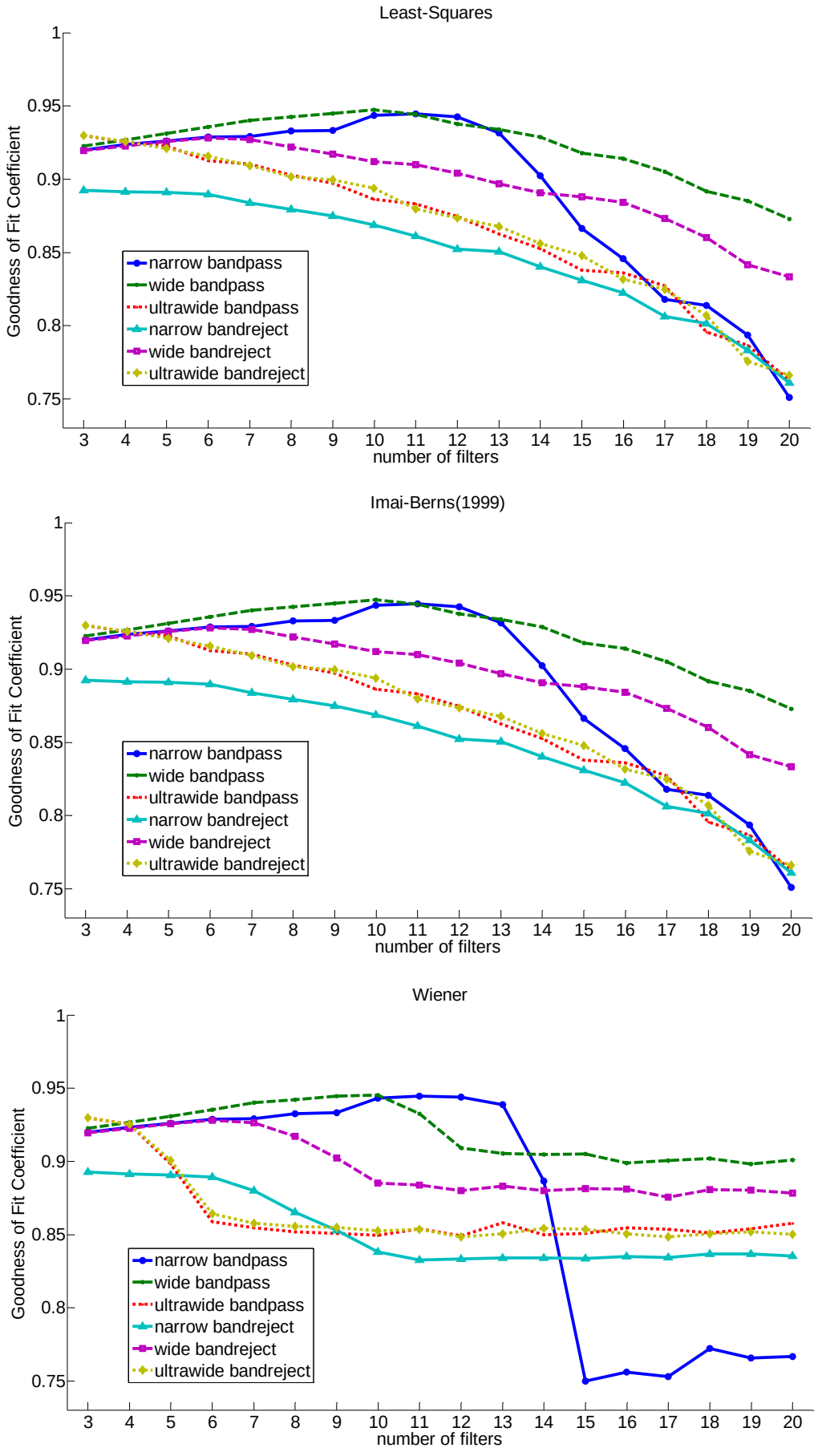

Figure 3: Accuracy of spectrum estimation evaluated by Goodness of Fit Coefficient (GFC).

Experimental results and discussion

As depicted by Figures 2 and 3, in general, the wide band-pass filter set consistently outperforms others, followed by its band-reject version. On the other hand, the pair of ultra-wideband filter sets results in similar and comparatively lower accuracy of reflectance estimation. Clearly the narrowband filters are not simply the best on all occasions as opposed to what Imai *et al.* concluded [4].

Surprisingly, the performance of the narrow band-pass filter sets varies significantly and decreases dramatically from 13-band onward suggested by both of the two metrics. Otherwise results of other filter sets shift rather smoothly.

Results obtained with the first and second methods illustrate very similar tendencies, whereas the Wiener estimation yields somewhat different results potentially due to the involvement of noise in the computation. As the number of bands increases, Wiener estimation tends to provide more stable results, whereas the performance of the other two methods reduces gradually, except of the narrow band-pass set.

The optimal number of filters largely depends on the methods used, and the two metrics do not seem to make a difference, however the metrics do change the order of performance. For instance, the narrow band-reject filter set is the worst method in terms of GFC, while it is not the case in terms of RMSE.

In our previous work [8] Mean Square Error was employed as the metric, which makes the results visually different from the ones presented here.

Conclusions

We evaluated the performance of 6 types of filters of varying bandwidths in terms of the accuracy of spectral reflectance estimation with three linear estimation methods in the context of multispectral image acquisition, with the help of a simulated imaging framework.

The results are not fully consistent with the conclusions drawn by previous work that narrow band-pass filters always yield higher spectral reproduction accuracy. Nevertheless, we found that band-pass and band-reject filters of reasonably wide band commonly seen in practice benefit multispectral acquisition. Further, band-pass or band-reject filters of extremely narrow or broad bandwidths perform unsatisfactorily or unsteadily.

The experiments were conducted in simulated lighting condition that is sufficient in terms of intensity. In insufficient lighting conditions, we assume that the advantages of wider bandwidths would be more visible in the system sensitivity as well as the signal-to-noise ratio.

Acknowledgement

The authors thank the Regional Council of Burgundy in France and Gjøvik University College in Norway for funding the research work collaboratively.

References

1. Bayer BE (1976), *Color Imaging Array*, Patent, US 3971065.
2. Parulski KA (1985), Color filters and processing alternatives for one-chip cameras, *IEEE Transactions on Electron Devices*, **32** (8), 1381-1389.
3. Primary color and complementary color filters, Digital camera Know-Hows, Lesson 29, Panasonic Corporation, [http://panasonic.jp/support/global/cs/dsc/knowhow/knowhow29.html – last accessed 7 November 2014].
4. Imai FH, Rosen MR and Berns RS (2000), Comparison of spectrally narrow-band capture versus wide-band with a priori sample analysis for spectral reflectance estimation, *Proceedings of the Eighth Color Imaging Conference*, 234-241, Scottsdale, USA.
5. Maestro2 Brochure, Thermo Fisher Scientific Inc., [http://www.thermofisher.com.au/ – last accessed 8 November 2014].
6. Wang X, Thomas JB, Hardeberg JY and Gouton P (2013), Median filtering in multispectral filter array demosaicking, *Proceedings of SPIE: Digital Photography IX*, 86600E-86600E-10, Burlingame, USA.
7. Wang X, Thomas JB, Hardeberg JY and Gouton P (2013), Discrete wavelet transform based multispectral filter array demosaicking, *Proceedings of the Colour and Visual Computing Symposium (CVCS) 2013*, 1-6, Gjøvik, Norway.
8. Wang X, Thomas JB, Hardeberg JY and Gouton P (2013), A study on the impact of spectral characteristics of filters on multispectral image acquisition, *Proceedings of the Twelfth Congress of the International Colour Association*, 1765-1768, Newcastle-Gateshead, UK.
9. Imai FH and Berns RS (1999), Spectral estimation using trichromatic digital cameras, *Proceedings of the International Symposium on Multispectral Imaging and Color Reproduction for Digital Archives*, 42-49.
10. Hironaga M and Shimano N (2010), Reflectance reconstruction for multispectral imaging by adaptive Wiener estimation, *Applied Optics*, **49** (31), 6140-6148.
11. Foster DH, Amano L, Nascimento SMC and Foster MJ (2006), Frequency of metamerism in natural scenes, *Journal of the Optical Society of America A*, **23** (10), 2359–2372.
12. Yasuma F, Mitsunaga T, Iso D and Nayar SK (2008), Generalized assorted pixel camera, *Technical Report*, Department of Computer Science, Columbia University.
13. Romero J, García-Beltrán A and Hernández-André J (1997), Linear bases for representation of natural and artificial illuminants, *Journal of the Optical Society of America A*, **14** (5), 1007-1014.